JTTEE5 18:90–95
DOI: 10.1007/s11666-008-9277-y
1059-9630/$19.00 © ASM International

Temperature Estimation and Al Content Prediction Focusing on Microstructural Change in a Thermal Barrier Coating

Mitsutoshi Okada, Tohru Hisamatsu, and Takayuki Kitamura

(Submitted March 24, 2008; in revised form June 18, 2008)

A superalloy with a thermal barrier coating (TBC) simulating a gas turbine blade is exposed to a high-temperature environment to develop a method for predicting the local temperature and Al content in a bond coat (BC). The Al content decreases with an increase in the test time due to the Al transport induced by the oxidation of the BC and the interdiffusion between the BC and the substrate. This brings about Al-decreased layer (ADL) at the boundary between the BC and the top coat. The thickness of the ADL increases in proportion to the square root of the test time, and the temperature dependence of the growth rate shows an Arrhenius-type behavior. Based on this relation, the local temperature of an in-service blade can be estimated by measuring the ADL thickness when the operation time is known. The Al content decreases in proportion to the ADL thickness. The prediction method of the Al content based on the relation is also presented.

Keywords Al content, bond coat, microstructural change, temperature, thermal barrier coating

1. Introduction

One way to improve the thermal efficiency of gas turbines in electric power generation is to increase the inlet gas temperature. As parts in hot-gas-path such as combustors, vanes, and blades are exposed to a high-temperature environment, thermal barrier coating (TBC) is applied to them to protect the metal substrate (Ref 1). The TBC as well as the internal cooling becomes increasingly important as the temperature increases. Owing to the reliability of the parts and the reduction in the maintenance cost, the development of a life evaluation method is inevitable.

There is no good method for measuring the surface temperature during the operation, even though it strongly affects the life. Therefore, it is important to develop an accurate method for estimating the temperature distribution. A method using the diameter of the γ' precipitate (Ref 2-5) was presented for Ni-base superalloys, which was widely used for turbine blades. A method based on the thickness of the oxide layer of the bond coat (BC) (thermally grown oxide, TGO) was also reported (Ref 6, 7). The TGO consists of Al-rich oxide layer and the mixed oxide of Al, Cr, Co, and Ni (Ref 8), and their growth rates are different. A method using the porosity of the top coat has a large estimation error at temperatures lower than 1273 K (Ref 9). An estimation method based on the thickness of the diffusion layer formed at the boundary between the corrosion-resistant coating (MCrAlY) and the substrate was also proposed (Ref 3, 10). Although several estimation methods based on the microstructural changes of substrates or coatings have been proposed (Ref 2-7, 9, 10), their accuracy has not been clarified.

Protective Al-rich oxide grows on the BC surface under a high-temperature oxidation environment (Ref 11-14). However, as the oxidation proceeds, the Al content in BC decreases due to the oxidation and interdiffusion with the substrate. The decrease in the Al content accelerates the oxidation when the protective oxide cannot be formed, and this promotes the TBC delamination. Therefore, the prediction of Al content is important for evaluating the life of TBC and gas turbine components.

This paper proposes a method for the estimation of the local temperature and discusses its estimation accuracy. A method for predicting the Al content in the BC is also examined.

2. Experimental Procedure

2.1 Specimen

Substrate bars of Inconel738LC, whose chemical composition is listed in Table 1 were prepared. The substrate bars have a diameter of 10 mm and a length of 150 mm, and they are cut into cylindrical specimens with a length of 20 mm. The BC of CoNiCrAlY (Co-32Ni-21Cr-8Al-0.5Y (wt.%)) with a thickness of 100 μm is formed on the side of the specimen by low pressure plasma spraying (LPPS).

Mitsutoshi Okada and **Tohru Hisamatsu**, Central Research Institute of Electric Power Industry, 2-6-1 Nagasaka, Yokosuka 240-0196, Japan; and **Takayuki Kitamura**, Department of Mechanical Engineering and Science, Kyoto University, Kyoto, Japan. Contact e-mail: mitutosi@criepi.denken.or.jp.

To protect the substrate from oxidation, CoNiCrAlY coating is also deposited on the top and bottom of the specimen by air plasma spraying (APS). Heat treatment is carried out after the spraying at 1393 K for 2 h and 1118 K for 24 h in a vacuum. Subsequently, top coat (TBC) of yttria partially stabilized zirconia (YSZ, 8 wt.%Y_2O_3-ZrO_2) with a thickness of 200 μm is deposited on the specimen by APS.

2.2 Exposure to High-Temperature Environment and Microstructure Observation

The specimens are exposed to constant temperatures of 1173, 1223, 1273, and 1323 K for a certain test time in air by using an electric tube furnace with an internal diameter of 70 mm. Before the test, the specimen is heated at a rate of 200 K/h, and the temperature fluctuation in the test section is maintained at approximately 2-3 K during the test. After the test, the specimen is cooled to approximately 773 K at a rate of 200 K/h and further to the room temperature inside the furnace without temperature control. The specimen is then cut at the center, and the cross section is ground for observation. No surface treatment such as etching is performed. The microstructure of the specimen is observed by means of an optical microscope and a scanning electron microscope (SEM). The BC microstructure is photographed by a CCD camera attached to the optical microscope. The microstructural change due to the oxidation is evaluated by a personal computer using the image processing software Win ROOF (Mitani Corp., Japan). The distribution of elements around the BC is analyzed, and the Al content in the BC is measured with an electron probe microanalyzer (EPMA).

Table 1 Chemical composition of Inconel738LC

C	Si	Mn	P	S	Ni	Cr	Mo	Co
0.09	0.02	0.01	<0.005	0.001	Bal.	16.00	1.70	8.48
W	**Al**	**Ti**	**Fe**	**Ta**	**Cu**	**Ag**	**Bi**	
2.54	3.52	3.45	0.06	1.74	<0.01	<0.5 ppm	<0.1 ppm	

3. Experimental Results and Discussion

3.1 Estimation of Temperature

Figure 1 shows the microstructural change in the BC at 1273 K. The boundary between the TBC and the BC has a roughness of approximately 10 μm, and the oxide (boundary oxide layer) grows along the boundary. The oxide thickness increases with the test time.

The BC originally comprises two phases; dark dots in bright mother phase as shown in Fig. 1(a). Figure 1(b) shows that the dark dots disappear near the TBC/BC boundary while they still exist at the BC/substrate boundary. Figure 2 shows the distribution of elements near the TBC/BC boundary before and after heating at 1223 K for 500 h observed with the EPMA. It clearly points out that the two phases are β-(Ni(Co), Al) and γ-(Co(Ni), Cr) rich. The authors compare the elemental distribution in this study with that reported in the previous studies (Ref 13, 15) to determine the phase constitution. Aluminum oxide is formed along the boundary. The low Al content region, namely, the ''Al-decreased layer (ADL),'' which is caused by the diffusion, is observed at the boundary between the oxide layer and two-phase microstructure in the BC. The ADL is determined as the layer where the β phase disappears, and its Al content is approximately 4 wt.%. The phase constitution of the ADL is identified as γ phase since it has a composition similar to that of the γ phase observed in a previous report (Ref 13). The composition of ADL does not vary with the test temperature and time.

Figure 3 shows the relationship between the ADL thickness and the square root of the test time. Four micrographs with a magnification of 500 are obtained at arbitrary positions in each specimen by means of an optical microscope with a CCD camera, and the ADL thickness is measured at three points in each micrograph

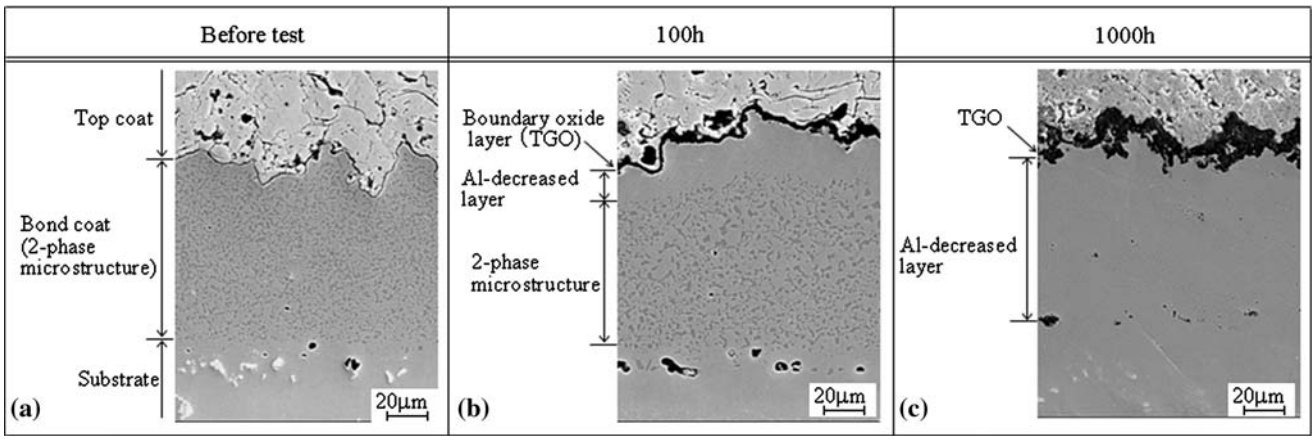

Fig. 1 Microstructural change of bond coat in TBC specimens at 1273 K in air (a) before test, (b) after 100 h, (c) after 1000 h

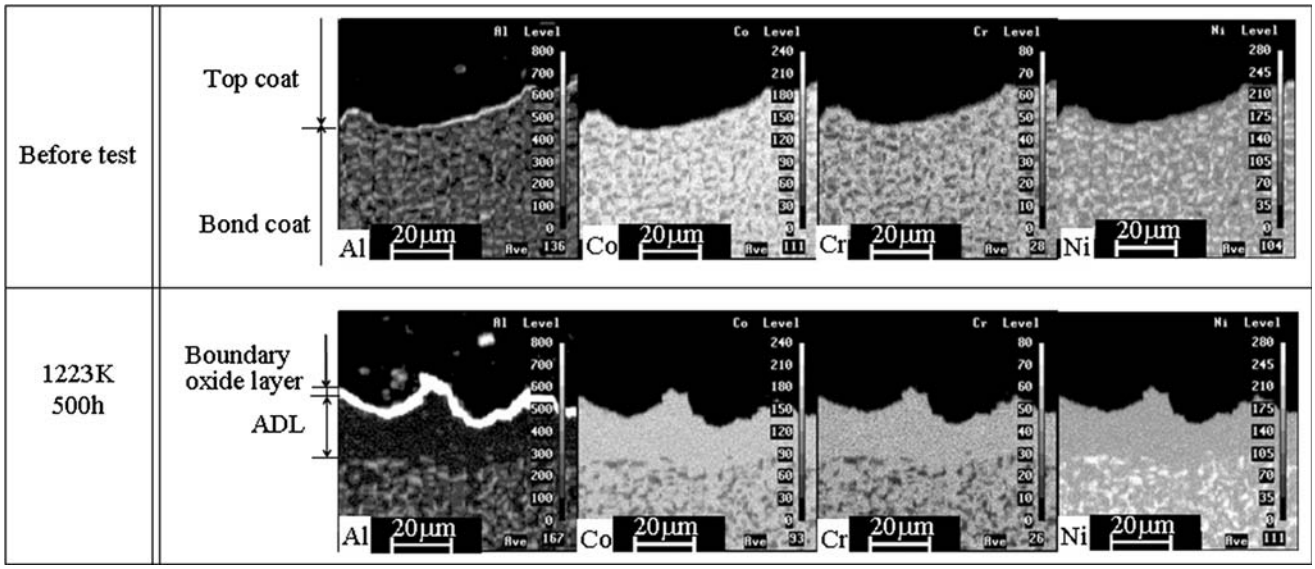

Fig. 2 Distribution of elements around the boundary between top coat and bond coat by means of EPMA before test and after 500 h at 1223 K

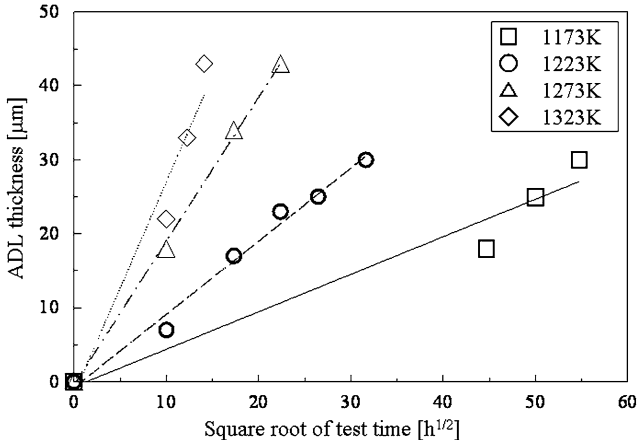

Fig. 3 Relationship between ADL thickness and square root of test time

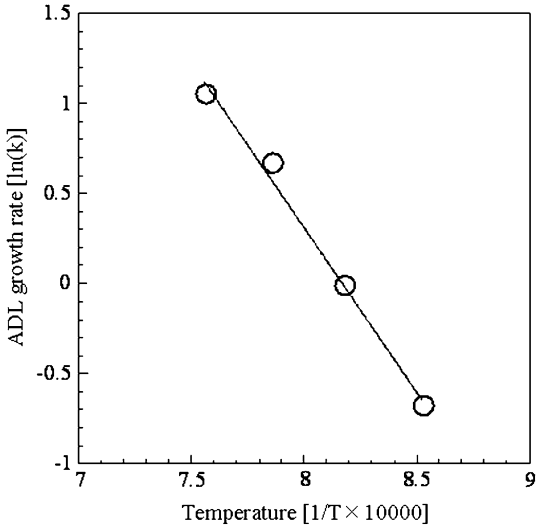

Fig. 4 Arrhenius plot of ADL growth rate

by the image processing software. For each specimen, the average of 12 data points is defined as the thickness. With regard to the scatter in the thickness of a specimen, the average square root of the unbiased variance is smaller than 10 μm under all the test conditions. The ADL thicknesses after 500 h at 1273 K and 200 h at 1323 K are eliminated in the figure since the ADL grows to the thickness of the bond coat as shown in Fig. 1(c). The relationship between the ADL thickness l (μm) and the test time t (h) is of the form

$$l = kt^{1/2} \qquad \text{(Eq 1)}$$

where k is a constant representing the growth rate. The value of k at each test temperature is evaluated by the least squares method. The Arrhenius plot shown in Fig. 4 indicates that

$$k = 2.96 \times 10^6 \exp\left(-\frac{152 \times 10^3}{RT}\right) \qquad \text{(Eq 2)}$$

where T and R are the temperature (K) and gas constant (8.31 J/(mol K)), respectively. Then, from Eq 1 and 2, T is expressed as follows:

$$T = \varphi(l,t) = -\frac{152 \times 10^3}{R} \cdot \frac{1}{\ln \frac{l}{2.96 \times 10^6 t^{1/2}}} \qquad \text{(Eq 3)}$$

Equation 3 enables us to estimate the temperature at the vicinity of the BC surface by measuring the ADL thickness at the hot section of the in-service component when the operation time is known.

The detection limit of the ADL obtained using an optical microscope is approximately 10 μm. This value is the minimum thickness of the layer since the thickness has a considerable scatter. On the other hand, the ADL that is larger than 50 μm coalesces with another ADL growing at the boundary between the BC and the substrate due to interdiffusion. The thickness cannot be determined when it is larger than approximately 50 μm. Thus, the ADL thickness from 10 to 50 μm is the applicable condition in the method. As the applicable limits depend on the temperature, the applicable operation time varies as shown in Fig. 5. Further, the scatter in the data caused due to the roughness on the BC surface, as shown in Fig. 1, also affects the accuracy.

Assuming that the error in the operation time can be neglected, the unbiased variance of temperature u_T^2 is expressed as follows (Ref 16):

$$u_T^2 = \left(\frac{\partial \varphi}{\partial l}\right)_0^2 \frac{u_l^2}{n} \quad \text{(Eq 4)}$$

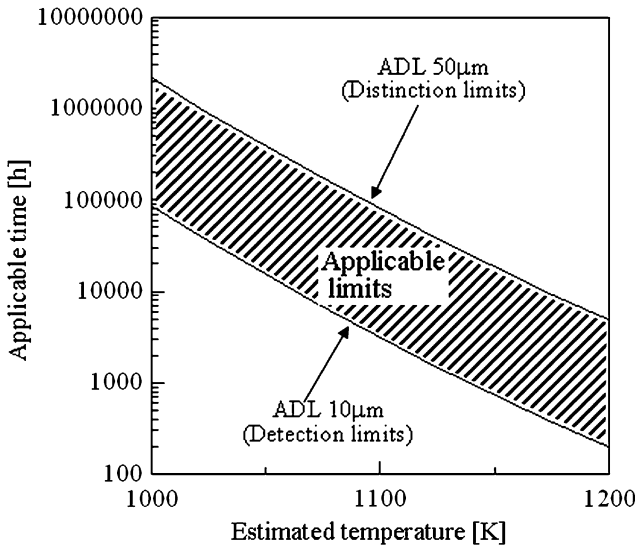

Fig. 5 Applicable limits of the temperature estimation method

Here, $\left(\frac{\partial \varphi}{\partial l}\right)_0$ is the differential of Eq 3 with respect to l. u_l and n are the square root of the unbiased variance of the ADL thickness and the number of the measurement, respectively. u_T varies with the temperature and time since the ADL thickness is their function. Figure 6 shows the relationship between the estimated temperature and its error (confidence coefficient 99%) where $u_l = 10$ and $n = 10$. The estimation error is smaller than 20 K in almost all the applicable limits.

3.2 Prediction of Al Content

Figure 7 shows the distribution of aluminum in the BC after 500 h at 1223 K observed by the EPMA where the electron probe is scanned from the top coat/BC boundary to the BC/substrate boundary. The distribution is not uniform since the BC has the two-phase microstructure

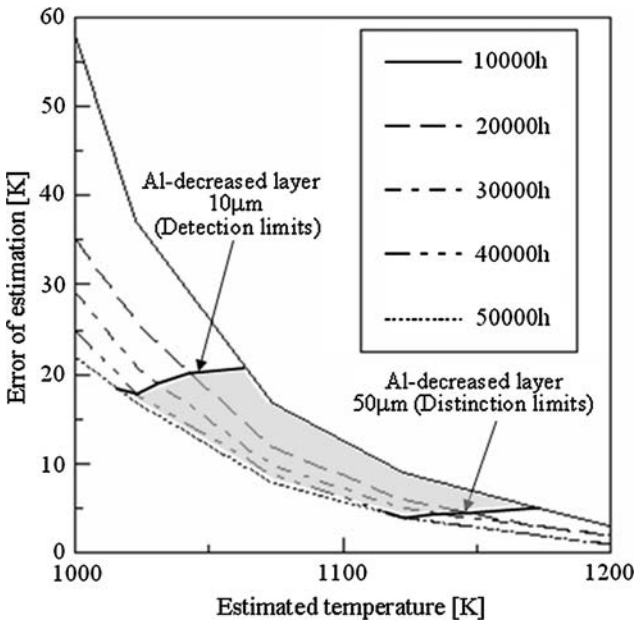

Fig. 6 Error of estimated temperature by means of ADL thickness (confidence coordinate 99%)

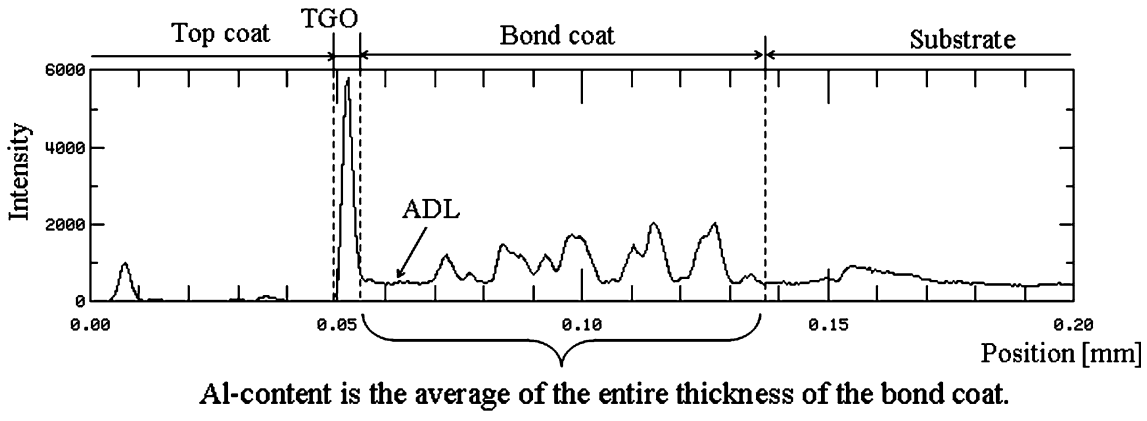

Fig. 7 Aluminum distribution in bond coat after 500 h at 1223 K in air

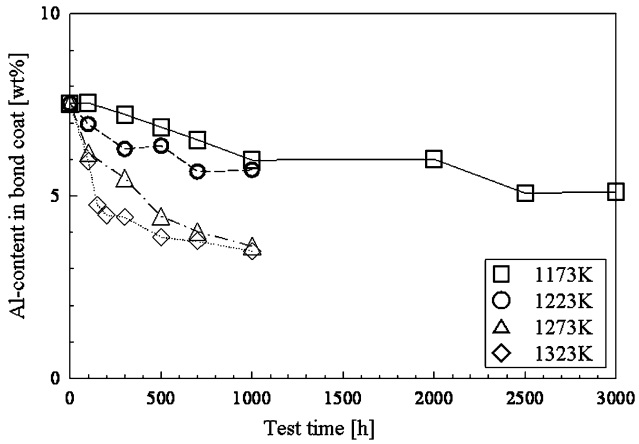

Fig. 8 Relationship between Al content in bond coat and test time

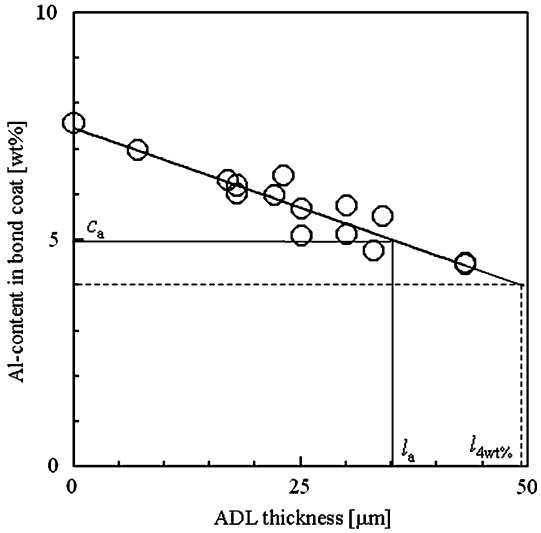

Fig. 9 Relationship between Al content in bond coat and ADL thickness

and ADL. The Al content in the BC is obtained using the relationship between the detected intensity and the content, which is acquired from the analysis of a standard sample, and using a special computer program for correction against absorption, fluorescence, and atomic number effects, and in this paper it is defined as the average of the entire BC thickness. Figure 8 shows the relationship between the Al content and the test time. The Al content is the average of four data points in each specimen. It decreases monotonously with an increase in the test time and temperature. Figure 9 shows the relationship between the Al content and the ADL thickness. The results after 500 h at 1273 K and after 200 h at 1323 K are eliminated since the ADL grows to the thickness of the BC. The Al content decreases in proportion to the ADL thickness. The Al content can be predicted based on this relation as follows. The ADL thickness at an arbitrary location of a gas turbine component is measured after the

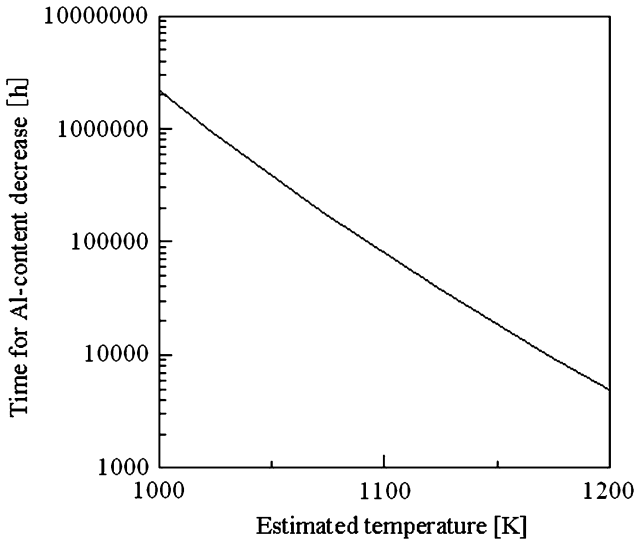

Fig. 10 Prediction of time for the decrease of Al content in bond coat (the time when Al content decreases to 4 wt.% is predicted)

operation. The local temperature can be predicted by the method mentioned above. From Fig. 9, the ADL thickness l_a corresponding to an arbitrary Al content c_a can be determined. The time taken to reach c_a can be calculated using Eq 1 and 2. Figure 10 shows the predicted time for the Al content to reach 4 wt.%.

4. Conclusion

High-temperature heating tests are conducted for the TBC specimens to develop methods to estimate the temperature and to predict the Al content on the basis of the microstructural change in a BC. The ADL is formed at the vicinity of the BC surface due to oxidation, and its thickness increases in proportion to the square root of the test time. The operation temperature can be estimated by measuring the thickness of the ADL on a blade of the in-service gas turbine on the basis of the relation among the thickness, time, and temperature. The applicable condition due to the thickness of BC and the detection limit of the ADL is given in Fig. 5. The error in the estimation due to the roughness on the BC surface is also evaluated.

The Al content of the BC is measured with an EPMA. The Al content decreases in proportion to the ADL thickness. Using this relationship, the time taken to reach an arbitrary Al content can be predicted.

References

1. A. Feuerstein, J. Knapp, T. Taylor, A. Ashary, A. Bolcavage, and N. Hitchman, Technical and Economical Aspects of Current Thermal Barrier Coating Systems for Gas Turbine Engines by Thermal Spray and EBPVD: A Review, *J. Therm. Spray Technol.*, 2008, **17**(2), p 199-213
2. J.M. Aurrecoechea, W.D. Brentnall, and J.R. Gast, Service Temperature Estimation of Turbine Blades Based on

Microstructural Observations, *J. Eng. Gas Turbines Power*, 1991, **113**(2), p 251-259
3. V. Srinivasan, N.S. Cheruvu, T.J. Carr, and C.M. O'Brien, Degradation of MCrAlY Coating and Substrate Superalloy During Long Term Thermal Exposure, *Mater. Manuf. Process.*, 1995, **10**(5), p 955-969
4. Y. Yomei, N. Okabe, D. Saito, K. Fujiyama, and T. Okamura, Service Temperature Estimation for Gas Turbine Buckets Based on Microstructural Change, *J. Soc. Mater. Sci. Jpn.*, 1996, **45**(6), p 699-704 (in Japanese)
5. A. Nomoto, M. Yaguchi, and T. Ogata, *Evaluation of Creep Properties of Directionally Solidified Nickel Base Superalloy for Gas Turbine Blades Based on Microstructures*, Central Research Institute of Electric Power Industry Report, T99094, Tokyo, Japan, 2000 (in Japanese)
6. M. Arai and U. Iwata, Temperature Estimation of Gas Turbine Combustor Based on Thermally Growth Oxidation Measurement in Thermal Barrier Coating, *Therm. Nucl. Power*, 2003, **54**(9), p 1064-1069 (in Japanese)
7. T. Torigoe, S. Aoki, I. Okada, and H. Koguma, Metal Temperature Estimation of High Temperature Components, Japan Patent JP.2003-4548, 2003 (in Japanese)
8. S. Takahashi, M. Yoshiba, and Y. Harada, Failure Analysis of High-Temperature Oxidation for Plasma Sprayed Thermal Barrier Coating Systems with Different Coating Characteristics, *Mater. Sci. Forum*, 2004, **461-464**, p 367-374
9. T. Fujii and T. Takahashi, Development of Operating Temperature Prediction Method Using Thermophysical Properties Change of Thermal Barrier Coatings, *J. Eng. Gas Turbines Power*, 2004, **126**, p 102-106
10. M. Okada, Y. Etori, T. Hisamatsu, and T. Takahashi, Temperature Estimation and Prediction of Aluminum-Content by Means of Microstructural Change in Gas Turbine Coatings, *J. Soc. Mater. Sci. Jpn.*, 2005, **54**, p 257-264 (in Japanese)
11. R.A. Miller, Oxidation-Based Model for Thermal Barrier Coating Life, *J. Am. Ceram. Soc.*, 1984, **67**, p 517-521
12. S. Bose and J. DeMasi-Marcin, Thermal Barrier Coating Experience in Gas Turbine Engines at Pratt & Whitney, *J. Therm. Spray Technol.*, 1997, **6**(1), p 99-104
13. A. Rabiei and G. Evans, Failure Mechanism Associated with the Thermally Grown Oxide in Plasma-sprayed Thermal Barrier Coatings, *Acta Mater.*, 2000, **48**, p 3963-3976
14. S. Takahashi, M. Yoshiba, and Y. Harada, Nano-Characterization of Ceramic Top-Coat/Metallic Bond-Coat Interface for Thermal Barrier Coating Systems by Plasma Spraying, *Mater. Trans.*, 2003, **44**(6), p 1181-1189
15. K. Noguchi, M. Nishida, and A. Chiba, Transmission Electron Microscopy of Low Pressure Plasma Sprayed CoNiCrAlY Coating, *Scr. Mater.*, 1996, **35**, p 1359-1364
16. Y. Yoshizawa, *New Theory of Error*, Kyoritsu-shuppan, Tokyo, Japan, 1989, p 157-161 (in Japanese)